Resistive relaxation in the field-induced insulator-metal transition of a $(La_{0.4}Pr_{0.6})_{1.2}Sr_{1.8}Mn_2O_7$ bilayer manganite single crystal

M. Matsukawa,[1,*] K. Akasaka,[1] H. Noto,[1] R. Suryanarayanan,[2] S. Nimori,[3] M. Apostu,[2]
A. Revcolevschi,[2] and N. Kobayashi[4]
[1]*Department of Materials Science and Technology, Iwate University, Morioka 020-8551, Japan*
[2]*Laboratoire de Physico-Chimie de L'Etat Solide, CNRS, UMR8648 Universite Paris-Sud, 91405 Orsay, France*
[3]*National Institute for Materials Science, Tsukuba 305-0047, Japan*
[4]*Institute for Materials Research, Tohoku University, Sendai 980-8577, Japan*
(Received 19 April 2005; published 5 August 2005)

We have investigated the resistive relaxation of a $(La_{0.4}Pr_{0.6})_{1.2}Sr_{1.8}Mn_2O_7$ single crystal, in order to examine the slow dynamics of the field-induced insulator-to-metal transition of bilayered manganites. The temporal profiles observed in remanent resistance follow a stretched exponential function accompanied by a slow relaxation similar to that observed in magnetization and magnetostriction data. We demonstrate that the remanent relaxation in magnetotransport has a close relationship with magnetic relaxation that can be understood in the framework of an effective-medium approximation by assuming that the first-order parameter is proportional to the second-order one.

DOI: 10.1103/PhysRevB.72.064412 PACS number(s): 75.47.Lx, 75.50.Lk

I. INTRODUCTION

The discovery of the colossal magnetoresistance (CMR) effect in doped manganites with perovskite structure has stimulated considerable interest for the understanding of their physical properties.[1] Though the insulator-to-metal (IM) transition and its associated CMR are well explained on the basis of the double-exchange (DE) model, it is pointed out that the dynamic Jahn-Teller (JT) effect due to the strong electron-phonon interaction plays a significant role in the appearance of CMR as well as the DE interaction.[2,3] Furthermore, Dagotto *et al.* propose a phase separation model where ferromagnetic (FM) metallic and antiferromagnetic (AFM) insulating clusters coexist as supported by recent experimental studies on the physics of manganites.[4]

The bilayer manganite $La_{1.2}Sr_{1.8}Mn_2O_7$ exhibits a paramagnetic insulator (PMI) to ferromagnetic metal (FMM) transition around $T_c \sim 120$ K and its associated CMR effect.[5] In comparison with cubic manganites, the MR effect of the compound under consideration, due to its layered structure, is enhanced by two orders of magnitude, at 8 T, around T_c. It is well known that Pr substitution on the La site leading to $(La_{1-z}Pr_z)_{1.2}Sr_{1.8}Mn_2O_7$ causes an elongation of the c-axis length in contrast with a shrinkage of the $a(b)$ axis, resulting in a change of the e_g-electron occupation from the $d_{x^2-y^2}$ to the $d_{3z^2-r^2}$ orbital.[6–8] These findings also accompany a variation of the easy axis of magnetization from the ab plane to the c axis. For the $z=0.6$ crystal, the field-induced FMM state is realized, instead of the PMI ground state in the absence of magnetic field. In Fig. 1, a phase diagram in the (M,T) plane, established from the magnetization measurements carried out on the $z=0.6$ crystal, with three regions labeled as the PMI, FMM, and mixed phases (hatched area) is presented.[10] A schematic diagram of free energy with two local minima corresponding to the PMI and FMM states is also given in Fig. 1, for the virgin state (a) before application of the magnetic field, the field-induced state (b) after the PMI to FMM transition, and the mixed state (c), after removal of the field. Just after removing the field, the system still remains in a metastable FMM state. After a long time, the system comes back to the original PMI state through the mixed state consisting of both FMM and PMI regions. In the mixed state, the total system is divided into a large number of subsystems which are randomly distributed, with different local densities of free energy, causing complex relaxation processes observed in the physical property studies.[11–16] A magnetic frustration between double-exchange ferromagnetic and superexchange antiferromagnetic interactions at the

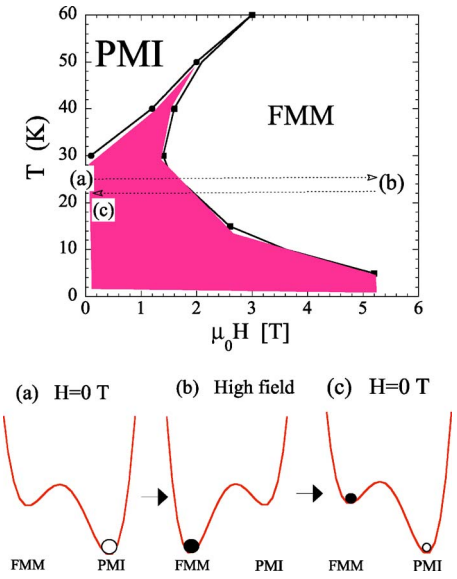

FIG. 1. (Color online) Magnetic phase diagram in the (H,T) plane established from the magnetic measurements carried out on the $z=0.6$ crystal. A schematic picture of the free energy with two local minima corresponding to the FMM and PMI phases [regions (a), (b), and (c) correspond to virgin state, field-induced metallic state, and mixed state, respectively].

Mn sites gives rise to a spin-glass-like behavior in manganites.[12,13,15] In the mixed phase, composed of metallic and insulating regions, it is believed that the resistive relaxations reported[11,14] arise from an electronic competition between double-exchange-like itinerancy and carrier localization associated with the formation of polarons. Recently, the slow dynamics of a remanent lattice striction of $(La_{0.4}Pr_{0.6})_{1.2}Sr_{1.8}Mn_2O_7$ single crystal has been examined on the basis of a competition between Jahn-Teller-type orbital lattice and DE interactions.[16] The former interaction induces a local lattice distortion of Mn O_6 octahedra along the c axis but the latter suppresses a lattice deformation through the itinerant state.[17] Thus it is desirable to establish a close relationship among the resistive, magnetic, and lattice relaxations, for our understanding of the CMR phenomena in bilayered manganites.

Hence we have investigated the resistive relaxation of a $(La_{0.4}Pr_{0.6})_{1.2}Sr_{1.8}Mn_2O_7$ single crystal. We compare our results with both magnetic and lattice relaxation data on the $z=0.6$ crystal.

II. EXPERIMENT

Single crystals of $(La_{0.4}Pr_{0.6})_{1.2}Sr_{1.8}Mn_2O_7$ were grown by the floating zone method using a mirror furnace. The calculated lattice parameters were shown in a previous report.[9] The dimensions of the $z=0.6$ sample are 3.4×3 mm^2 in the ab plane and 1 mm along the c axis. Magnetoresistance was measured by means of a conventional four-probe technique at the Tsukuba Magnet Laboratory, the National Institute for Materials Science and at the High Field Laboratory for Superconducting Materials, Institute for Materials Research, Tohoku University. Magnetostriction measurements were performed using a strain gauge method.[16] The magnetization measurements were made using a superconducting quantum interference device magnetometer at Iwate University.

III. RESULTS AND DISCUSSION

Let us show in Fig. 2 the magnetoresistance data R_{ab} of single crystalline $(La_{0.4},Pr_{0.6})_{1.2}Sr_{1.8}Mn_2O_7$ at selected temperatures. First, a field-induced insulator-to-metal transition and its associated CMR effect are observed around 2 T, accompanied by a huge decrease in resistance by about two orders of magnitude. Second, a clear hysteresis in R_{ab} is seen, even though applied fields are lowered down to zero. As mentioned above, the system still remains in a metastable state just after the external field is switched off. In Fig. 2(a), it can be seen that the characteristic field which switches the sample state from PMI to FMM, depends upon temperature and increases from 1.8 T at 30 K to 2.2 T at 20 K, in good agreement with the magnetization curves in the inset of Fig. 2(a). Moreover, such a critical field is also controlled by changing an applied current [Fig. 2(b)]. A local joule heating assists numerous PMI clusters within the sample to jump over potential barriers of local free energy, allowing them to shift from PMI towards FMM states, resulting in a suppression of both the switching field and hysteresis effect. Here, we estimate a volume fraction of metal (or insulator) from

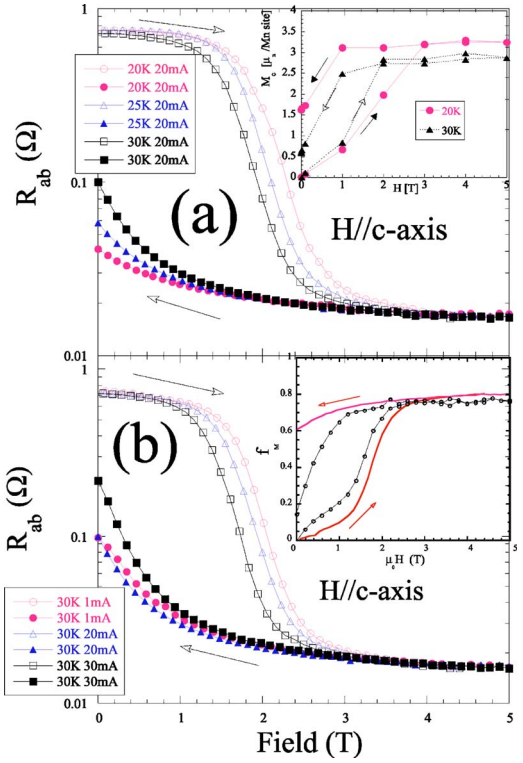

FIG. 2. (Color online) Magnetoresistance data R_{ab} of a $(La_{0.4}Pr_{0.6})_{1.2}Sr_{1.8}Mn_2O_7$ single crystal in a field applied along the c axis, (a) at $T=20$, 25, and 30 K for $I=20$ mA and (b) at $I=1$, 20, and 30 mA for 30 K. The inset of (a) shows the field dependence of the magnetization along the c axis at both 20 and 30 K. In the inset of (b), a solid curve represents the volume fraction of metal phase f_M estimated from the $R(H)$ data using an effective-medium approximation discussed in the text. For comparison, the normalized magnetization curve $M(H)/M_{full}$ at 30 K is also presented.

the $R(H)$ data using an effective-medium approximation (EMA).[18,19] In our calculation, we assume a two-component composite material made up of both metallic and insulating grains with their resistivities, ρ_M and ρ_I, giving an effective resistivity ρ_e for spherical shape as follows:

$$f_M\frac{\rho_e-\rho_M}{\rho_e+2\rho_M}+(1-f_M)\frac{\rho_e-\rho_I}{\rho_e+2\rho_I}=0, \tag{1}$$

where f_M denotes a volume fraction of metal with metallic resistivity ρ_M. Substituting the $R(H)$ data into the above equation and solving it with respect to f_M, we get a volume fraction of metal as shown in the inset of Fig. 2(b). For comparison, the magnetization curve at 30 K is also presented. The calculated curve based on the EMA roughly reproduces the $M(H)$ curve, except for the low-field region in the demagnetization process. The difference in $M(H)$ and f_M is probably related to the formation of magnetic domains conserving ferromagnetic moments.[20] Another reason for the difference is reduced to the EMA approximation, which is a rough approximation based on the spherical shapes. Here, ρ_I is taken as the value of R just before application of the field and ρ_M is determined from the value of $R(H)$ at a maximum field of 5 T. Furthermore, a volume fraction of metallic clus-

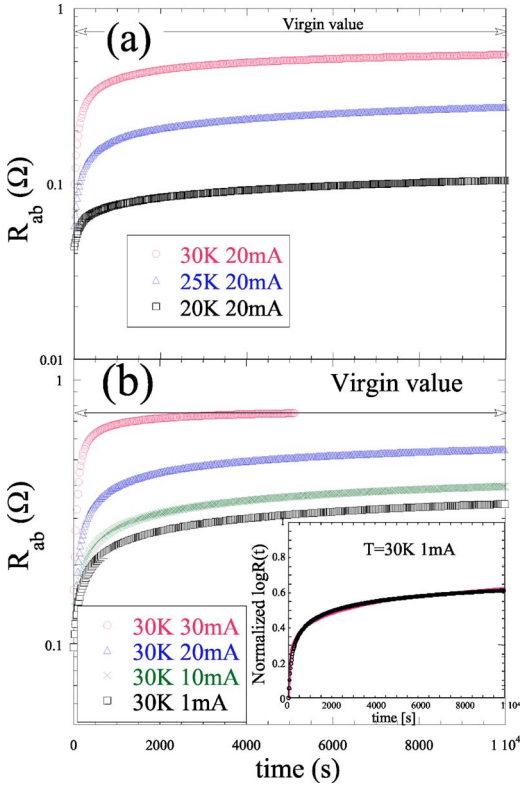

FIG. 3. (Color online) Resistive relaxation profiles of a $(La_{0.4}Pr_{0.6})_{1.2}Sr_{1.8}Mn_2O_7$ single crystal as a function of (a) temperature and (b) current. (a) $I=1$, 10, 20, and 30 mA at 30 K, (b) $T=20$, 25, and 30 K at $I=30$ mA. The inset of (b) represents a typical curve fitted to normalized $\log_{10}R(t)$ data at 30 K with $I=1$ mA, using a stretched exponential function with characteristic relaxation time and exponent, τ and β, respectively. We have $\tau=1.1\times10^4$ s and $\beta=0.25$.

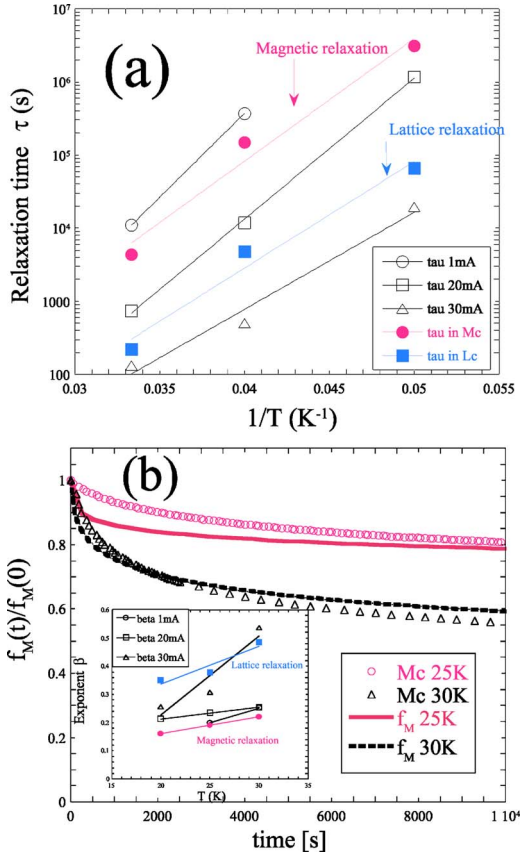

FIG. 4. (Color online) (a) Resistive relaxation time τ_R as a function of $1/T$ for $I=1$, 20, and 30 mA. For comparison, both the magnetic and lattice relaxation parameters, τ_M and τ_L, are also given. (b) A relaxation profile of the metallic fraction f_M estimated from the $R(t)$ data using the EMA model. Solid and dashed curves represent calculation data at 25 and 30 K, respectively. The normalized c-axis magnetization data, $M_c(t)/M_c(0)$, are given. In the inset of (b), the exponent β in the resistive, magnetic, and lattice relaxations is plotted as a function of temperature.

ter at 5 T is assumed to be equal to the ratio $M(5\text{ T})/M_{full}=\sim0.8$, in which M_{full} means the value of full magnetization corresponding to the magnetic moment of the Mn ion ($=3.4\mu_B$ at a hole content $x=0.4$). According to a previous work on cubic manganites by Jaime *et al.*,[21] assuming both ferromagnetic and electronic free-energy functionals and minimizing the total free energy, a solution is obtained where the first-order parameter m $[=M(H,T)/M_{full}]$ is proportional to the second-order parameter c $(=f_M)$. Thus it is reasonable to take the preceding assumption in the EMA.

Now, we examine the resistive relaxation data as a function of temperature and excited current, as depicted in Figs. 3(a) and 3(b). The system starts from a metastable state of the coexistence between metallic and insulating regions when a field is turned off, and should come back to a stable insulator at the original ground state after a very long time. At 30 K, the value of R_{ab}, with $I=30$ mA, rapidly relaxes within a few hundred seconds and then restores the ground-state value, as shown in Fig. 3. The relaxation time of remanent R_{ab} is elongated at least by two orders of magnitude upon decreasing temperature from 30 K down to 20 K. We have noted from previous studies that a relaxation curve in both remanent magnetization and lattice striction in single crystalline $(La_{0.4}Pr_{0.6})_{1.2}Sr_{1.8}Mn_2O_7$ is well fitted using a stretched exponential function with the characteristic relaxation time and exponent, τ and β. A deviation in exponent from $\beta=1$ indicates the existence of multiple relaxation processes in the observed slow dynamics. In a similar way, we try to examine a temporal profile of remanent magnetoresistance following a stretched exponential form such as normalized $\log_{10}R(t)=[\log_{10}R(t)-\log_{10}R(0)]/[\log_{10}R(\infty)-\log_{10}R(0)]=1-\exp[-(t/\tau)^\beta]$, where $R(\infty)$ and $R(0)$ denote the virgin and initial values, before application of the field and just after removal of the field, respectively. A typical curve fitted to normalized $R(t)$ data at 30 K $I=1$ mA is presented in the inset of Fig. 3(b).

As a result, the fitted parameters τ_R and β are plotted as a function of temperature, as shown in Fig. 4. For comparison, the previous relaxation parameters, τ_M and τ_L, for both magnetization and magnetostriction curves, are also given. First, upon decreasing the applied current, the value of τ_R tends to approach the magnetic relaxation time τ_M. This tendency is also observed in the temperature variation of exponent β, as shown in the inset of Fig. 4(b). On the other hand, the value of τ_L is smaller by about two orders of magnitude than the lifetime of $R(t)$ and $M(t)$. Second, the relaxation time in $R(t)$, $M(t)$, and $L(t)$ follows the thermally activated T dependence,

$\tau = \tau_0 \exp(\Delta/kT)$, where Δ denotes the activation energy corresponding to the potential barrier between the metastable FMM state and the local maximum in free energy. τ_0 represents the intrinsic relaxation time determined from microscopic mechanism. The activation energy of $R(t)$, Δ_R, varies from 305 K at $I=30$ mA, through 443 K at $I=20$ mA, up to 530 K at $I=1$ mA. These values are not far from the activation energies of both remanent lattice and magnetization, $\Delta_L=335$ K and $\Delta_M=386$ K. The resistive and magnetic relaxations are taken as signatures of the phase transition from metastable FMM to stable PMI states in the long time scale. On the other hand, the lattice relaxation is not due to the structural transition associated with cooperative phenomena but arises from a local lattice distortion of MnO_6 octahedra, without a long-range order. In Fig. 4(b), a temporal profile of the metallic fraction f_M estimated from the $R(t)$ data for $I=1$ mA using the EMA model is given. We notice that calculated curves of the metallic fraction tend to approach the magnetization data after a long period of time. This finding seems to be reasonable if we assume that a ferromagnetic order parameter m is proportional to an electronic one, $f_M \rightarrow c$. The difference in the initial drop between the metallic fraction and the magnetization curves is probably related to the formation of FMM domains which might be responsible for the disagreement observed between f_M and the normalized magnetization, as depicted in the inset of Fig. 2(b).

Finally, we explore resistive relaxation data as a function of field at selected temperatures, as shown in Fig. 5. The value of the relaxation time grows exponentially upon increasing the applied field because a local minimum in the free energy of the metastable state is stabilized by lowering the minimum free energy by $\mu_{eff}\mu_0 H$. The field dependence of $\tau(H)$ is well fitted by a function such as $\tau_R(0)\exp(\mu_{eff}\mu_0 H/kT)$. The effective magnetic moment μ_{eff} is expressed as $\mu_{eff}=Ng\mu_B S$, giving the average number N of the Mn ions, contributing to the relaxation process of the FMM to PMI transition at the level of clusters in divided subsystems.[11] Here, S represents the average spin number at the Mn ion site and we set $S=1.8$ at a hole concentration of 0.4. A characteristic size of FMM clusters is estimated, from the relaxation data using the above exponential function to be equal to $N_R=140$ at 30 K ($N_R=166$ at 25 K). Moreover, from magnetic $\tau(H)$ we get $N_M=122$ at 30 K, similar to the value of N_R. If the average distance between adjacent Mn ions is taken as 4 Å, the cluster size of the FMM region reaches several degrees of nanometers. On the other hand, τ_L is independent of field up to 0.5 T and shows no outstanding variation, in contrast with the value of both $\tau_R(H)$ and $\tau_M(H)$. This finding indicates that magnetostriction phenomena are not always associated with a long-range-order parameter although magnetization and magnetotransport are closely related to it.

In summary, we have shown that the field-induced insulator-to-metal transition observed in the single crystalline $(La_{0.4}Pr_{0.6})_{1.2}Sr_{1.8}Mn_2O_7$ is accompanied by a resistive relaxation process. The temporal profiles observed in remanent resistance follow a stretched exponential function accompanied by a slow relaxation similar to those exhibited by magnetization and magnetostriction. We demonstrate that the remanent relaxation in magnetotransport has a close relationship with the magnetic relaxation that can be understood within the framework of an effective-medium approximation assuming a proportionality between the first-order parameter and the second-order one.

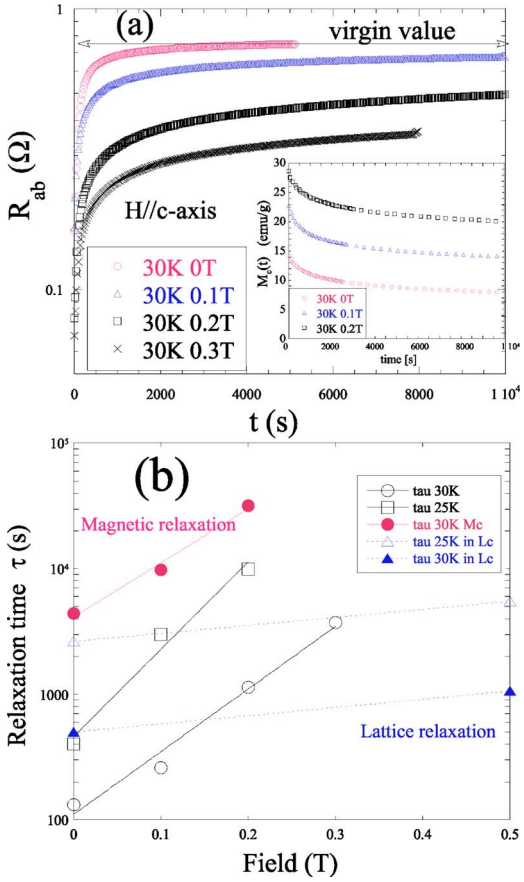

FIG. 5. (Color online) (a) Resistive relaxation profiles of a $(La_{0.4}Pr_{0.6})_{1.2}Sr_{1.8}Mn_2O_7$ single crystal as a function of field. $H=0$, 0.1, 0.2, and 0.3 T at 30 K with $I=30$ mA. In the inset of (a), magnetic relaxation data are also shown at 30 K. (b) The resistive relaxation time $\tau_R(H)$ as a function of field at 25 and 30 K with $I=30$ mA. For comparison, the magnetic and lattice relaxation times, $\tau_M(H)$ and $\tau_L(H)$, are also given at selected temperatures.

ACKNOWLEDGMENTS

This work was partially supported by a Grant-in-Aid for Scientific Research from the Ministry of Education, Science and Culture, Japan. The authors thank Emeritus Prof. K. Yoshida for his valuable discussion and Dr. H. Ogasawara for his technical support.

*Electronic address: matsukawa@iwate-u.ac.jp

[1] *Colossal Magnetoresistive Oxides*, edited by Y. Tokura (Gordon and Breach, New York, 2000).
[2] C. Zener, Phys. Rev. **82**, 403 (1951); P. G. deGennes, *ibid.* **118**, 141 (1960).
[3] A. J. Millis, P. B. Littlewood, and B. I. Shraiman, Phys. Rev. Lett. **74**, 5144 (1995); A. J. Millis, B. I. Shraiman, and R. Mueller, *ibid.* **77**, 175 (1996).
[4] For a recent review, see E. Dagotto, T. Hotta, and A. Moreo, Phys. Rep. **344**, 1 (2001).
[5] Y. Moritomo, A. Asamitsu, H. Kuwahara, and Y. Tokura, Nature (London) **380**, 141 (1996).
[6] Y. Moritomo, Y. Maruyama, T. Akimoto, and A. Nakamura, Phys. Rev. B **56**, R7057 (1997).
[7] H. Ogasawara, M. Matsukawa, S. Hatakeyama, M. Yoshizawa, M. Apostu, R. Suryanarayanan, G. Dhalenne, A. Revcolevschi, K. Itoh, and N. Kobayashi, J. Phys. Soc. Jpn. **69**, 1274 (2000).
[8] F. Wang, A. Gukasov, F. Moussa, M. Hennion, M. Apostu, R. Suryanarayanan, and A. Revcolevschi, Phys. Rev. Lett. **91**, 047204 (2003).
[9] M. Apostu, R. Suryanarayanan, A. Revcolevschi, H. Ogasawara, M. Matsukawa, M. Yoshizawa, and N. Kobayashi, Phys. Rev. B **64**, 012407 (2001).
[10] M. Apostu, Ph.D. thesis, Université of Paris-Sud (2002).
[11] A. Anane, J. P. Renard, L. Reversat, C. Dupas, P. Veillet, M. Viret, L. Pinsard, and A. Revcolevschi, Phys. Rev. B **59**, 77 (1999).
[12] M. Uehara and S. W. Cheong, Europhys. Lett. **52**, 674 (2000).
[13] J. Lopez, P. N. Lisboa-Filho, W. A. C. Passos, W. A. Ortiz, F. M. Aruajo-Moreira, O. F. de Lima, D. Schaniel, and K. Ghosh, Phys. Rev. B **63**, 224422 (2001).
[14] J. Dho, W. S. Kim and N. H. Hur, Phys. Rev. B **65**, 024404 (2001).
[15] I. Gordon, P. Wagner, V. V. Moshchalkov, Y. Bruynseraede, M. Apostu, R. Suryanarayanan, and A. Revcolevschi, Phys. Rev. B **64**, 092408 (2001).
[16] M. Matsukawa, M. Chiba, K. Akasaka, R. Suryanarayanan, M. Apostu, A. Revcolevschi, S. Nimori, and N. Kobayashi, Phys. Rev. B **70**, 132402 (2004).
[17] M. Medarde, J. F. Mitchell, J. E. Millburn, S. Short, and J. D. Jorgensen, Phys. Rev. Lett. **83**, 1223 (1999).
[18] D. A. G. Bruggeman, Ann. Phys. **24**, 636 (1935).
[19] D. J. Bergmann and D. Stroud, Solid State Phys. **46**, 147 (1993).
[20] Y. Tokunaga, M. Tokunaga, and T. Tamegai, Phys. Rev. B **71**, 012408 (2005).
[21] M. Jaime, P. Lin, S. H. Chun, M. B. Salamon, P. Dorsey, and M. Rubinstein, Phys. Rev. B **60**, 1028 (1999).